

Nonmelanoma Skin Cancers: Embryologically Relevant Sites and UV Exposure

Giovanni Nicoletti, MD,

FEBoPRAS*†

Marco Mario Tresoldi, MD*‡

Alberto Malovini, MS, PhD§

Borelli Francesco, MD¶

Angela Faga, MD, FICS†

Background: Traditionally, nonmelanoma skin cancers (NMSCs) are considered mainly UV-related malignancies. Nevertheless, a strong correlation between the embryologically relevant sites (ERS) of the head and neck and the preferential sites of onset of basal cell carcinomas (BCCs) has long been supposed and demonstrated. The aim of this research was the investigation of the potential correlation between the ERS of the head and neck and the sites of tumor onset in all of the NMSCs.

Methods: The distribution of 1165 NMSC was correlated with the ERS of the head and neck using the universally accepted anatomical diagrams featuring the congenital head and neck clefts and an original anatomical diagram showing the most credited sites of the embryonic fusion planes of the auricle.

Results: In our sample, both BCC and SCC display an increased likelihood of onset in the ERS of the head and neck. A proportion of 93.10% BCCs was distributed within ERS, while 6.90% derived from non-embryologically relevant sites ($P < 0.001$). A proportion of 69.70% SCCs was distributed within ERS, while 30.30% derived from non-embryologically relevant sites ($P < 0.001$). The probability of tumors within ERS was significantly higher for BCC versus SCC ($P < 0.001$), with BCCs having a 5-fold increase in the probability of occurring in ERS compared to SCCs ($P < 0.001$).

Conclusions: The ERS might host areas of cellular instability yielding to the development of an NMSC. The environmental UV exposure plays a relatively main role versus dysontogenic factors in the pathogenesis of SCC. (*Plast Reconstr Surg Glob Open* 2020;8:e2683; doi: [10.1097/GOX.0000000000002683](https://doi.org/10.1097/GOX.0000000000002683); Published online 7 April 2020.)

INTRODUCTION

Traditionally, nonmelanoma skin cancers (NMSCs) are considered mainly UV-related malignancies with an increased incidence in the elderly, where frequently there is evidence of damage from chronic sun exposure.¹ Chronic trauma,² scars,³ chronic wounds,⁴ X-ray⁵ and arsenic exposure,⁶ and immunodeficiency⁷ are also associated with the onset of NMSCs.

A growing number of literature reports have been disclosing the correlation between the embryonic fusion

planes of the head and neck and the preferential sites of onset of basal cell carcinomas (BCCs). Our research group already provided evidence of such a correlation⁸ and recently extended the investigation to the auricle,⁹ a traditionally neglected anatomical site in this research field.

The aim of this research was the investigation of the potential correlation between the embryonic fusion planes of the head and neck and the sites of onset in all of the NMSCs.

MATERIALS AND METHODS

An overall number of 947 patients with 1,165 histologically demonstrated NMSCs of the head and neck including the auricle were admitted at the Plastic and Reconstructive Surgery Unit of the University of Pavia, Istituti Clinici Scientifici Maugeri, Pavia (Italy), over a period of 10 years, from June 2008 to May 2018. Within the latter sample, 811 patients suffered from 1,000 BCCs and 136 patients suffered from 165 SCCs.

Multiple lesions from individual patients were considered as separate cases as the single skin tumor was considered the experimental unit of the study. For each patient, data on gender, age at the time of surgery, and localization of the tumor were recorded.

Disclosure: The authors have no financial interest to declare in relation to the content of this article.

From the *Plastic and Reconstructive Surgery, Department of Clinical Surgical, Diagnostic and Pediatric Sciences, University of Pavia, Pavia, Italy; †Advanced Technologies for Regenerative Medicine and Inductive Surgery Research Center, University of Pavia, Pavia, Italy; ‡Department of Surgery, Istituti Clinici Scientifici Maugeri, Pavia, Italy; §Laboratory of Informatics and Systems Engineering for Clinical Research, Istituti Clinici Scientifici Maugeri Research and Care Institute, Pavia, Italy; ¶Plastic, Reconstructive and Aesthetic Surgery Residency Program, Universities of Milan-Pavia, Pavia, Italy.

Received for publication July 24, 2019; accepted January 14, 2020.

Copyright © 2020 The Authors. Published by Wolters Kluwer Health, Inc. on behalf of The American Society of Plastic Surgeons. This is an open-access article distributed under the terms of the [Creative Commons Attribution-Non Commercial-No Derivatives License 4.0 \(CCBY-NC-ND\)](https://creativecommons.org/licenses/by-nc-nd/4.0/), where it is permissible to download and share the work provided it is properly cited. The work cannot be changed in any way or used commercially without permission from the journal.

DOI: [10.1097/GOX.0000000000002683](https://doi.org/10.1097/GOX.0000000000002683)

All of the cases underwent medical preoperative digital photography, and the records were stored in the Unit's dedicated master file.

The archived digital images were coded according to the specific location of each tumor according to its approximate center using the following diagrams identifying the sites of embryonic fusion planes, considered as embryologically relevant sites (ERS):

1. The original anatomic diagram of the Tessier classification of the craniofacial clefts¹⁰ (Fig. 1) where

the clefts are numbered from 0 to 14, with the lower numbers (0 to 7) representing the facial clefts and the higher numbers (8 to 14) representing their cranial extensions up to the lower half of the forehead. This classification was integrated by the anatomic diagram by Moore et al. featuring the paths of the "hairline indicators" of the craniofacial clefts that represent the superior and lateral extension of the Tessier original craniofacial cleft classification (Fig. 2).¹¹

2. A detailed original anatomical diagram featuring the typical sites of the congenital clefts, fistulas, and

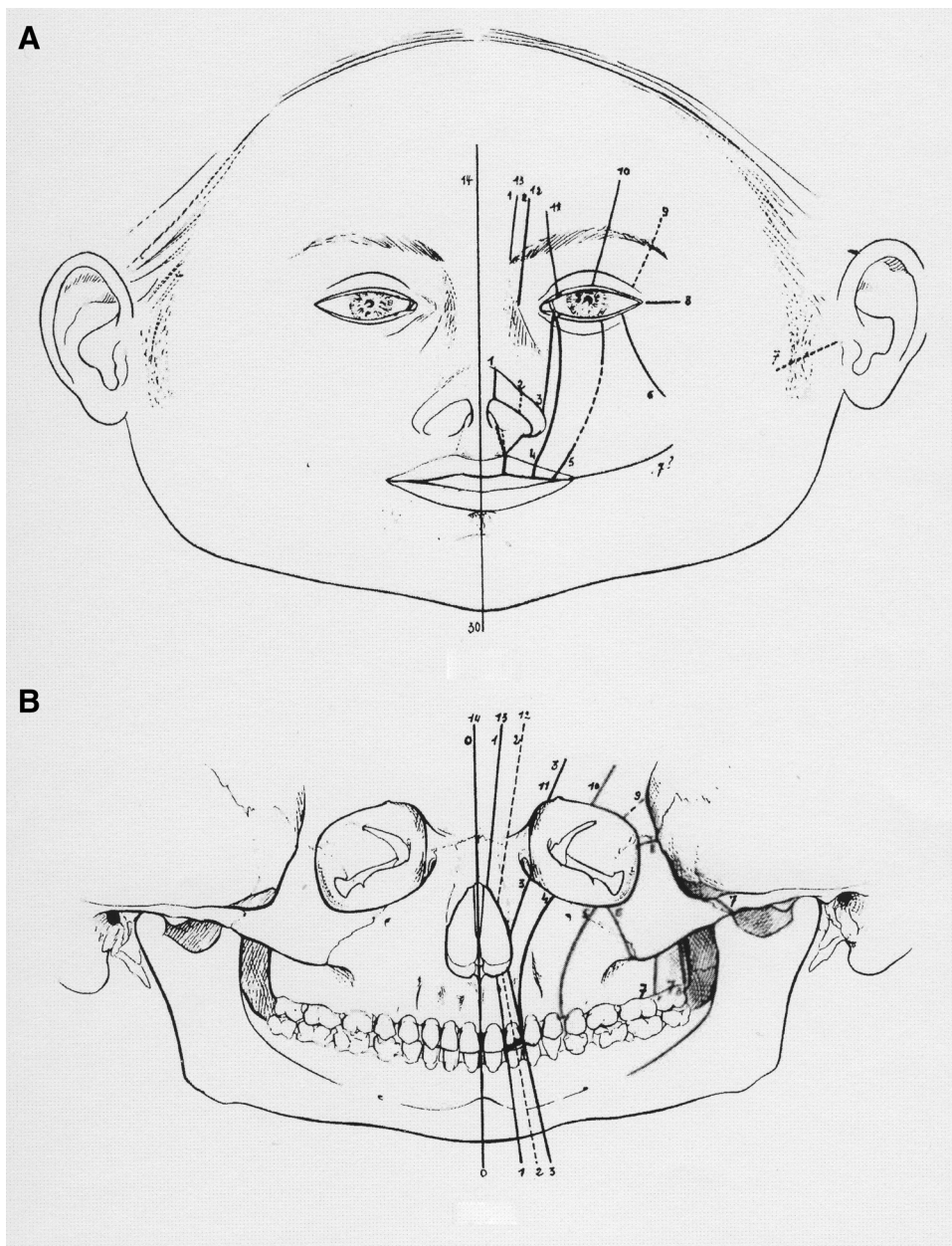


Fig. 1. The original Tessier anatomical diagram of craniofacial clefts: localization on (A) the soft tissues and (B) skeleton. The dotted lines are either uncertain localizations or uncertain clefts. Reprinted with permission from Elsevier: Tessier P. Anatomical classification facial, craniofacial and latero-facial clefts. *J Maxillofac Surg.* 1976;4:69–92.

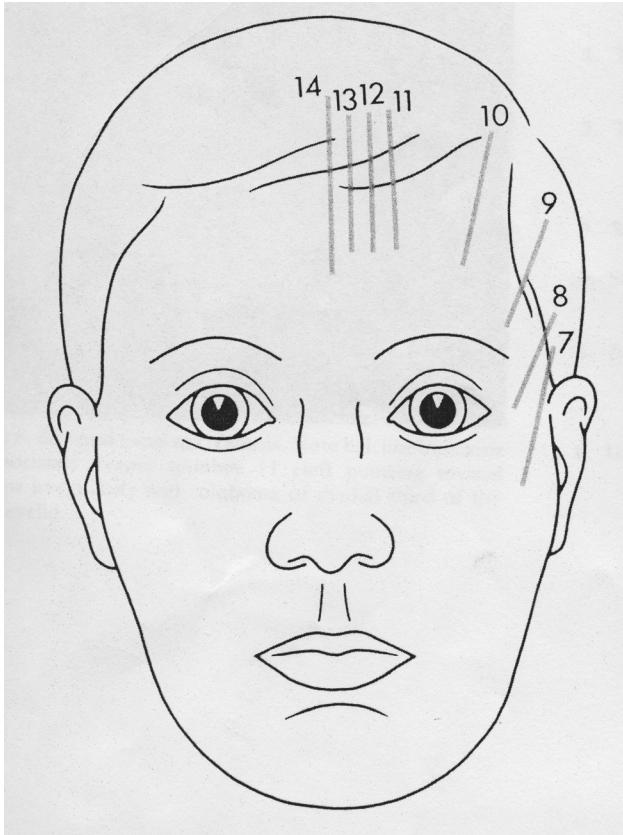


Fig. 2. Diagram featuring the hairline indicators representing the superior and lateral extensions of the Tessier original craniofacial cleft classification. Reprinted with permission from Wolters Kluwer Health: Moore MH, David DJ, Cooter RD. Hairline indicators of craniofacial clefts. *Plast Reconstr Surg.* 1988;82:589–593 ©1988 Wolters Kluwer Health.

cysts of the neck corresponding to 2 lines running along the sterno-cleido-mastoid muscle, from the mastoid to the jugular notch, and the anterior midline, from the chin to the jugular notch, respectively (Fig. 3).^{12–15}

3. An original full-size anatomical diagram derived from the reports by Streeter, Wood-Jones, Park, Porter and Minoux showing the 2 currently most credited sites of the embryonic fusion planes of the auricle.⁹ The planes were represented by two 5-mm-wide ribbon-like areas: the first one, termed hyoid-mandibular fusion plane (HM-FP), running along a line from the upper margin of the tragus towards the concha and then deflecting towards the lower margin of the tragus; the second one, termed free ear fold-hyoid fusion plane (FEFH-FP), running from the cranial-most portion of the helix to the mid-portion of the ascending helix (Fig. 4).⁹

All of the cases within each histological type were aggregated into 2 groups: the first including all of the tumors sitting on the ERS and the second one including all of the tumors sitting out of the former sites comprehensively termed non-embryologically relevant sites (nERS).

The first group (ERS) was then divided in 19 subgroups corresponding to:

- On the face, the sites of the Tessier classification of craniofacial clefts except for the clefts numbers 1 and 2 that were gathered into a single subgroup as their exact projection on the overlying soft tissue is virtually undistinguishable (15 subgroups).
- On the neck, the latero-cervical line and the anterior neck midline, the latter corresponding to the Tessier cleft number 30 (2 subgroups).
- On the auricle, the hyoid-mandibular fusion plane (HM-FP) and the free ear fold-hyoid fusion plane (FEFH-FP) (2 subgroups).

The second group (nERS) was also divided into 9 subgroups corresponding to the functional-esthetic subunits of the face and neck: forehead, eyelid, cheek, nose, ear, upper lip, lower lip, chin, and neck.^{16,17}

The number of tumor records was calculated for each group and subgroup.

Formal, informed written consent was obtained from all of the patients and the study conformed to the Declaration of Helsinki.

Statistical Methods

The exact binomial test was applied to test if the frequency of BCC and SCC tumors localized within ERS was significantly different from the fraction of tumors on ERS expected by chance (50%). The Shapiro–Wilk test was applied to test whether the distribution of age at surgical intervention deviated significantly from the normal distribution ($P < 0.05$). Age at surgical explant of BCC and SCC samples localized within ERS versus nERS and between ERS was compared by the nonparametric 2-sided Wilcoxon rank-sum test and by the Kruskal–Wallis test, respectively. The presence of statistically significant differences in terms of gender distribution between tumors within ERS versus nERS was evaluated by the 2-sided Fisher’s exact test for count data (when comparing gender distribution between ERS, P values were simulated by imposing 1,000,000 Monte Carlo replicates). The probability of tumors in BCC versus SCC sites was compared by the Pearson χ^2 test and by logistic regression. The significance threshold was set to $P < 0.05$. Statistical analyses were performed by the R statistical software v.3.5.1 (www.r-project.org).

RESULTS

Cohort Characteristics

A total number of 1,000 BCC samples from 811 patients and 165 SCC samples from 136 patients were analyzed. The main characteristics of the analyzed sample are reported in Table 1.

Distribution of BCC and SCC tumors

Figure 5, Figure 6, and Table 2 report the distribution of BCC and SCC samples by ERS and nERS.

- Of the 1,000 BCC samples analyzed, 931 (93.10%) were distributed within ERS, the remaining 69 (6.90%) derived from nERS: the proportion of BCC in ERS was significantly higher than 50%, the proportion of BCC

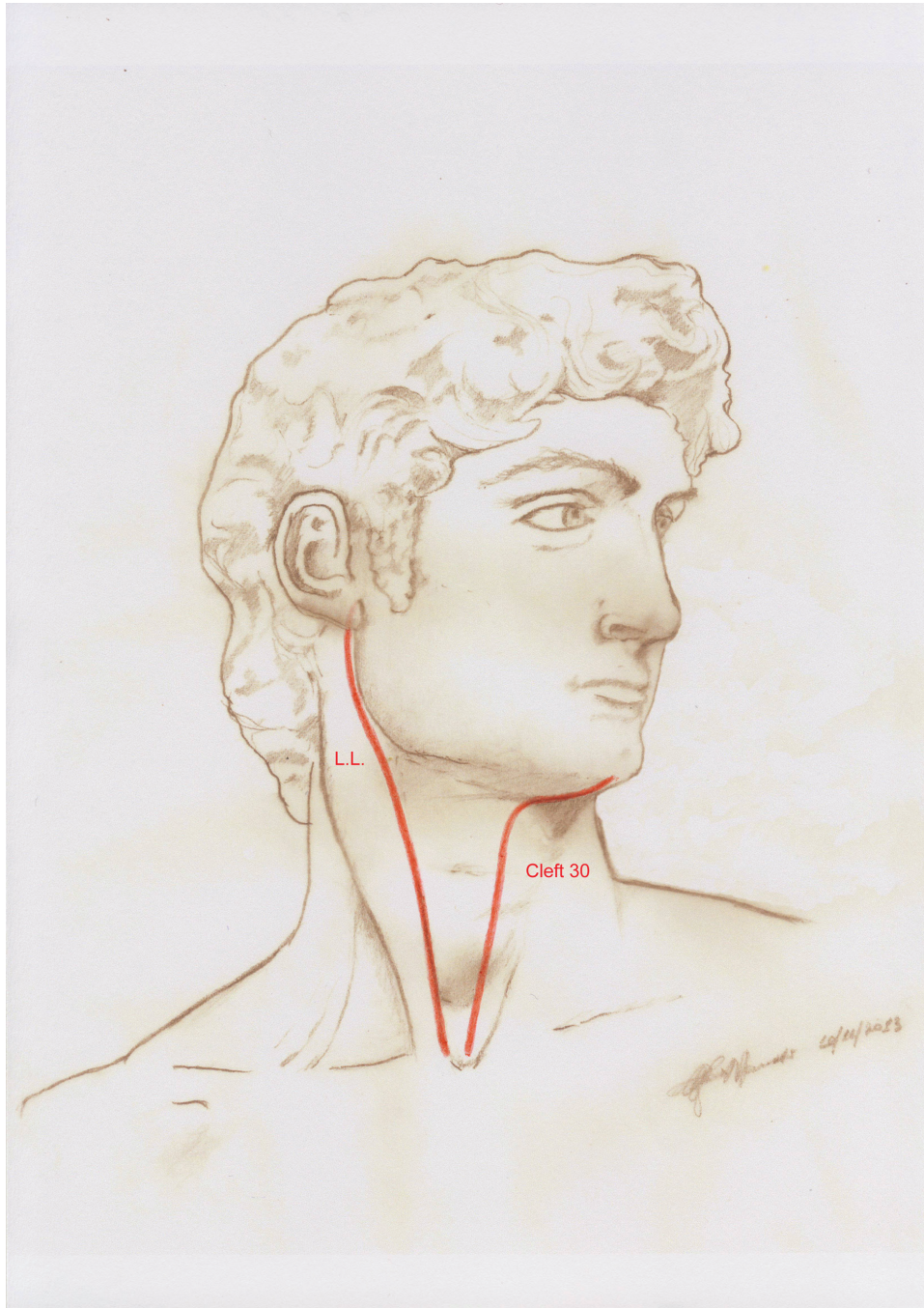


Fig. 3. Anatomical original diagram featuring the typical sites of congenital clefts, fistulas, and cysts of the neck: the laterocervical line (L.L.) and the anterior neck midline (Tessier cleft number 30). Reprinted with permission from Wolters Kluwer Health: Nicoletti G, Brenta F, Malovini A, Jaber O, Faga A. Sites of basal cell carcinomas and head and neck congenital clefts: topographic correlation. *Plast Reconstr Surg.* 2014; 2(6): e164. ©2014. The Author(s).

- localized in ERS expected by chance (95%, CI 91.35%–94.59%, $P < 0.001$) (Table 2).
- The proportion of BCC tumors from men and women was equally localized between ERS and nERS ($P = 0.059$), while unbalanced among specific ERS ($P = 0.004$) and nERS ($P = 0.046$) (Table 3).
 - The median age at surgical intervention for BCC was not different when localized in ERS compared to nERS ($P = 0.115$) but differed among specific ERS ($P < 0.001$) (Table 3).
 - Of the 165 SCC samples analyzed, 115 (69.70%) were distributed within ERS, the remaining 50 (30.30%)



Fig. 4. Original anatomical diagram showing the sites of the embryonic fusion planes of the auricle according to Streeter, Wood Jones, Park, Porter, and Minoux. The hyoid-mandibular fusion plane (HM-FP) is featured in red, and the free ear fold-hyoid fusion plane (FEFH-FP) in blue. Reprinted with permission from SAGE Publications Ltd.: Nicoletti G, Tresoldi MM, Malovini A, Prigent S, Faga A. Correlation between the sites of onset of basal cell carcinoma and the embryonic fusion planes in the auricle. *Clinical Medicine Insights: Oncology*. 12(1): 1–5, 2018.

derived from nERS: the proportion of SCC in ERS was significantly higher than 50%, the proportion of SCC localized in ERS expected by chance (95% CI, 62.07%–76.60%, $P < 0.001$) (Table 2).

- SCC tumors analyzed were more likely to be localized in ERS when deriving from women than from men (78.57% versus 63.16%, $P = 0.040$). Gender distribution was significantly different also across ERS localizations ($P < 0.001$) and nERS ($P = 0.003$) (Table 4).
- The median age at surgical intervention for SCC was not different when localized in ERS compared to nERS ($P = 0.376$) neither among ERS ($P = 0.225$) nor among nERS ($P = 0.518$) (Table 4).

The probability of tumors within ERS was significantly higher for BCC compared to SCC (93.10% versus 69.70%, $P < 0.001$), with BCCs having a 5-fold increase in the probability of occurring in ERS compared to SCCs adjusting for age and gender (odds ratio = 5.32, 95% CI, 3.43–8.25, $P < 0.001$).

Table 1. Characteristics of the Analyzed Sample

	BCC	SCC
Tumors	1,000	165
Patients	811	136
Gender		
Men	554 (55.40%)	95 (57.58%)
Women	446 (44.60%)	70 (42.42%)
Age (years)	74 (65–80)	82 (76–86)

Data are presented as counts (frequency, %) or median (25th–75th percentiles).

DISCUSSION

The carcinogenic role of UV radiation has long been demonstrated within the NMSCs.¹ Acute and chronic exposure to UV radiation promotes a deregulated proliferation of skin cells through genomic changes in all of the 3 stages of photo-carcinogenesis initiation, promotion, and progression.¹⁸ Besides the direct molecular damage, the carcinogenic effects of UV radiation are also related to immune system impairment yielding to survival and proliferation of abnormal cells and oncogenic viruses.⁷ The well-known carcinogenic effect of arsenic exposure, too, is attributable to immunosuppression through a direct action on lymphocytes including chromosomal and DNA abnormalities, decreased T-cell receptor activation, and the cellular status of oxidation and methylation.⁶

Similarly, the carcinogenic effects of chronic trauma, impaired wound healing and X-ray exposure are related to molecular damage of nucleic acids.^{2–5}

A favorite distribution of several skin proliferative diseases along embryological migration pathways has long been referred to the so-called Blaschko lines, supposed to trace the migration of embryonic cells.^{19,20} Recently, an increased tumor density was demonstrated within the embryonic fusion plane of the face.²¹

Our research group already provided evidence of a correlation between the sites of onset of BCCs and both the head and neck congenital clefts and the embryological fusion planes of the auricle.^{8,9}

The present study demonstrated that NMSCs display a significantly increased likelihood of onset in the ERS of the head and neck, with a preference for the anatomical sites most frequently affected by congenital clefts, as the Tessier's clefts numbers 1, 2, and 3. Nevertheless, within the NMSC group, a relevant difference was appreciated between BCCs and SCCs as the former tumor demonstrated a 5-fold likelihood of onset on an ERS versus the latter. Such a prevalence is likely to be related to the BCC's specific anatomical-pathological features, making BCC a unique and *sui generis* tumor.

Since 1948, BCC has been proposed as a “nevroid” tumor derived from pluripotential, dormant embryonal cells that somehow become activated later in life.²² Actually, BCCs constantly preserve the basic feature of adnexal primordia in the skin, established by stroma-associated proliferating epithelia.^{23,24}

Therefore, as highlighted by Pinkus, BCC should be differentiated from other pure epithelial malignancies featuring a cancer transformation of individual epithelial cells progressing to a typical stroma-dissociated

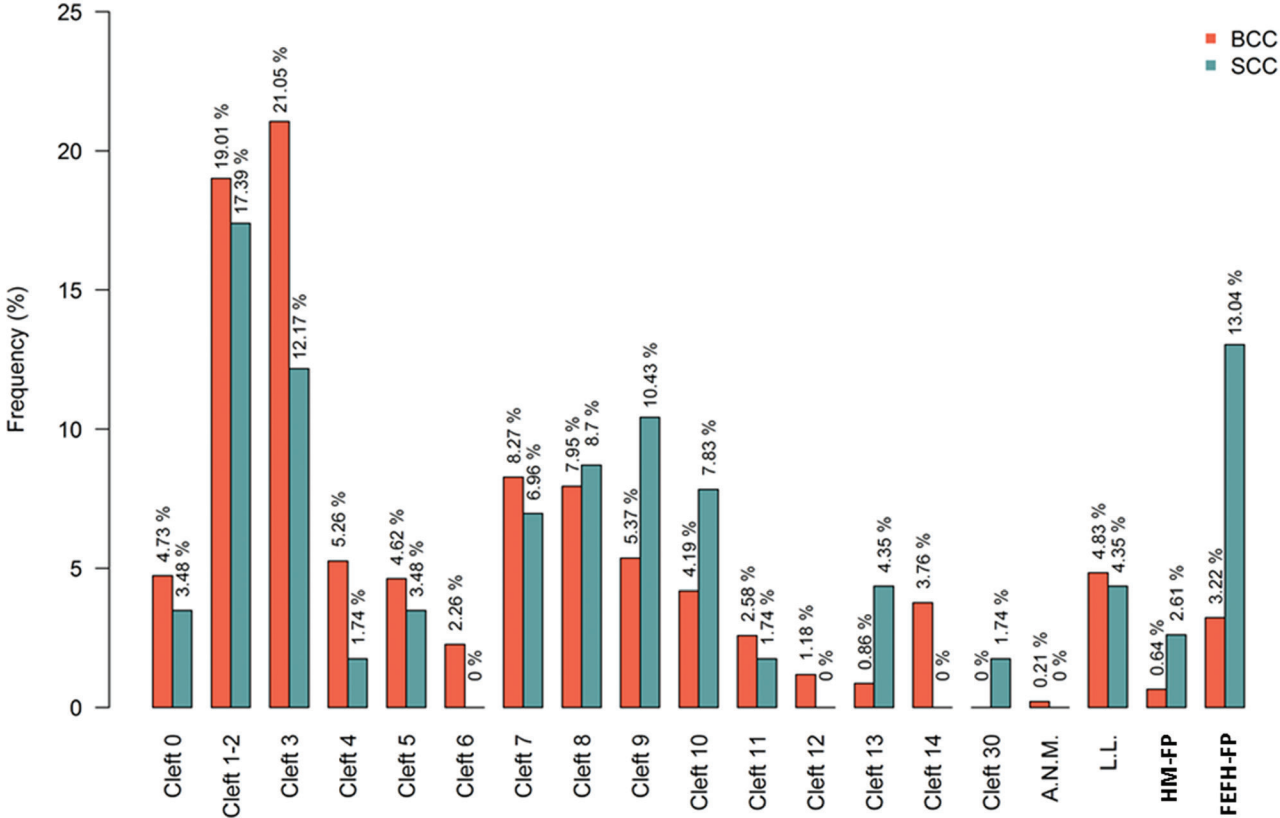


Fig. 5. Tumors distribution by ERS.

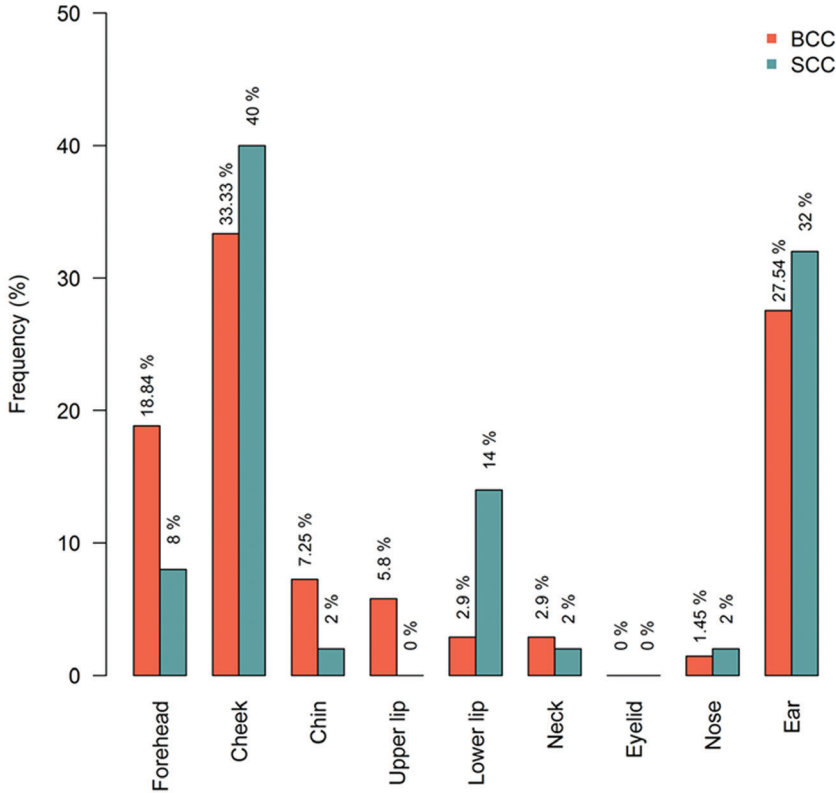


Fig. 6. Tumors distribution by non-embryologically relevant sites.

Table 2. Embryologically Relevant Sites (ERS): Specific Sites Distribution

Distribution	BCC Tumors N (%)	SCC Tumors N (%)
Within ERS/total tumors	931/1,000 (93.10)*	115/165 (69.70)*
By specific ERS/total within ERS		
Cleft 0	44 (4.73)	4 (3.48)
Cleft 1–2	177 (19.01)	20 (17.39)
Cleft 3	196 (21.05)	14 (12.17)
Cleft 4	49 (5.26)	2 (1.74)
Cleft 5	43 (4.62)	4 (3.48)
Cleft 6	21 (2.26)	0 (0.00)
Cleft 7	77 (8.27)	8 (6.96)
Cleft 8	74 (7.95)	10 (8.70)
Cleft 9	50 (5.37)	12 (10.43)
Cleft 10	39 (4.19)	9 (7.83)
Cleft 11	24 (2.58)	2 (1.74)
Cleft 12	11 (1.18)	0 (0.00)
Cleft 13	8 (0.86)	5 (4.35)
Cleft 14	35 (3.76)	0 (0.00)
Cleft 30	0 (0.00)	2 (1.74)
Anterior neck midline (A.N.M.)	2 (0.21)	0 (0.00)
Laterocervical line (L.L.)	45 (4.83)	5 (4.35)
HM-FP	6 (0.64)	3 (2.61)
FEFH-FP	30 (3.22)	15 (13.04)
By specific nERS/total within nERS		
Forehead	13 (18.84)	4 (8.00)
Cheek	23 (33.33)	20 (40.00)
Chin	5 (7.25)	1 (2.00)
Upper lip	4 (5.80)	0 (0.00)
Lower lip	2 (2.90)	7 (14.00)
Neck	2 (2.90)	1 (2.00)
Eyelid	0 (0.00)	0 (0.00)
Nose	1 (1.45)	1 (2.00)
Ear	19 (27.54)	16 (32.00)

*Pvalue given by the exact binomial test < 0.001.

Site, analyzed site; tumors distribution, count and frequency (%) of BCC and SCC tumors by site. FEFH-FP, fee ear fold-hyoid fusion plane; HM-FP, hyoid-mandibular fusion plane.

invasiveness.²⁵ This BCC's basic fibro-epithelial organized interdependent growth might be rather explained as a monstrous attempt at adnexogenesis in postnatal life, thus directing the question for pathogenesis to embryogenesis.

Recently, the time-honored hypothesis of a dysembryogenic pathogenesis of BCC was further supported by the evidence of an aberrant reactivation of the Hedgehog pathway in the development of a number of human malignancies including BCCs with relevant therapeutic innovations.^{26–29} Furthermore, anomalies in the Hedgehog signaling pathway were also demonstrated to play a relevant role in congenital craniofacial disease.^{30,31}

In our experience, within the ERS, SCCs demonstrated a preference for the area superior and lateral to the orbit, corresponding to the Tessier's clefts numbers 8, 9, 10, and 13, while, within the embryologically nonrelevant sites (nERS), they preferably affected the auricle, the cheek and the lower lip. In the latter site, the etiology has long been related to the long-term exposure to oncogenic substances.¹⁸ In the auricle and cheek, being sites with highest sun exposure, UV radiation undoubtedly plays the main role inducing DNA alterations, through genetic dysregulation of thymine dimers, N-ras oncogene, and p53 tumor suppressor gene.³²

Our study correlated the sites of onset of NMSC with the currently most credited and universally accepted mapping of the ERS of the head and neck. Undoubtedly,

a more comprehensive understanding of the interaction between dysontogenic and environmental factors in the pathogenesis of NMSC would be allowed by the correlation of our sample with a most accurate and universally credited mapping of the UV exposure of the head and neck, too. The currently available mapping of the different degrees of sun exposure in the head and neck do not provide the suitable level of accuracy, thus preventing the equally accurate double check between the embryologically and the environmentally relevant sites (Fig. 7).^{33,34}

Nevertheless, although the UV exposure plays a key role in the development of all skin cancers, our study demonstrates that all of the NMSCs preferably rise in ERS irrespective of their matching to the sites of highest sun exposure of the head and neck. Therefore, it might be supposed that UV exposure more likely triggers genetic dysregulation on potential dormant cell clusters with a prenatal proliferative setting localized within the ERS.

Interestingly, a significant difference in the age of onset was appreciated in BCCs versus SCCs. In BCCs, an earlier age of onset was appreciated in the Tessier's cleft number 3, that is the most frequent of all clefts, too, while no difference in age of onset was demonstrated for specific locations within the ERS in SCCs. In our opinion, such an evidence would confirm the relevance of dysembryogenic factors versus cumulative UV exposure in the pathogenesis of BCC.

Our study also demonstrated a different gender distribution in BCCs versus SCCs within the ERS: in BCCs, no difference in distribution was appreciated between women and men, while an SCC was more likely to grow in an ERS in the women. Such an evidence might be correlated to a wider use of sun-block creams in women, with a relative increase of dysembryogenic factors due to a reduction of the environmental ones in this sample. On the other hand, in men, traditionally less familiar with sun protection cosmetics in this age group, the oncogenic environmental factors would overwhelm the dysembryogenic ones in the pathogenesis of SCC with development of such a cancer in both ENR and nERS.

The recognition of the role of dysembryogenic factors in the pathogenesis of BCC allowed for the development of a novel noninvasive approach in the treatment of this skin tumor, based on specific Hedgehog pathway inhibitors.³⁵

According to our results, such an approach might be extended to the prevention of the development and/or progression of the SCC, too.

The identification of preferential anatomical sites of onset of NMSCs might be relevant to guide the today's general plastic reconstructive surgery practitioner in making a proper diagnosis when facing an early poorly defined skin lesion. Furthermore, such a knowledge might suggest a higher level of caution when planning elective locally invasive procedures within these areas.

CONCLUSIONS

The anatomical sites corresponding to the embryonic fusion planes might host areas of cellular instability

Table 3. BCC Tumors: Gender and Age Distribution by Site

	BCC Tumors		P	Age Median (IQR)	P
	Gender				
	Women	Men			
Overall			0.059		0.115
Within ERS	423 (94.84)	508 (91.70)		74 (65–80)	
Within nERS	23 (5.16)	46 (8.30)		76 (68–83)	
By ERS			0.004*		< 0.001#
Cleft 0	18 (4.26)	26 (5.12)		73 (63–77.25)	
Cleft 1–2	77 (18.2)	100 (19.69)		75 (67–81)	
Cleft 3	107 (25.3)	89 (17.52)		70 (58–79)	
Cleft 4	24 (5.67)	25 (4.92)		72 (64–79)	
Cleft 5	25 (5.91)	18 (3.54)		71 (65–81.5)	
Cleft 6	10 (2.36)	11 (2.17)		74 (65–81)	
Cleft 7	32 (7.57)	45 (8.86)		76 (69–83)	
Cleft 8	29 (6.86)	45 (8.86)		75 (69.25–80.75)	
Cleft 9	21 (4.96)	29 (5.71)		75.5 (60–80.75)	
Cleft 10	12 (2.84)	27 (5.31)		71 (55–76)	
Cleft 11	10 (2.36)	14 (2.76)		73 (63.75–80.75)	
Cleft 12	8 (1.89)	3 (0.59)		69 (60–76)	
Cleft 13	5 (1.18)	3 (0.59)		74 (62.25–79)	
Cleft 14	22 (5.20)	13 (2.56)		76 (70–83)	
Cleft 30	0 (0.00)	0 (0.00)		—	
Anterior neck midline (A.N.M.)	1 (0.24)	1 (0.20)		69 (68–70)	
Laterocervical line (L.L.)	14 (3.31)	31 (6.10)		77 (72–80)	
HM-FP	1 (0.24)	5 (0.98)		75 (68.75–82)	
FEFH-FP	7 (1.65)	23 (4.53)		78 (73.25–84)	
By nERS			0.046*		0.603
Forehead	6 (26.09)	7 (15.22)		72 (66–76)	
Cheek	10 (43.48)	13 (28.26)		75 (69–83)	
Chin	1 (4.35)	4 (8.70)		68 (66–78)	
Upper lip	2 (8.70)	2 (4.35)		83 (72.25–88.25)	
Lower lip	2 (8.70)	0 (0.00)		82.5 (80.75–84.25)	
Neck	0 (0.00)	2 (4.35)		76.5 (70.25–82.75)	
Eyelid	0 (0.00)	0 (0.00)		—	
Nose	0 (0.00)	1 (2.17)		75 (75–75)	
Ear	2 (8.70)	17 (36.96)		77 (72.5–81.5)	

* $P < 0.05$; # $P < 0.001$. Gender analyses: Women, count (%) of women with BCC in a specific site; men, count (%) of men with BCC in a specific site. Age analyses: site, median (25th–75th percentiles) of age distribution in specific sites. FEFH-FP, free ear fold-hyoid fusion plane; HM-FP, hyoid-mandibular fusion plane.

Table 4. SCC Tumors: Gender and Age Distribution by Site

	SCC Tumors		P	Age Median (IQR)	P
	Gender				
	Women	Men			
Overall			0.040*		0.376
Within ERS	55 (78.57)	60 (63.16)		82 (76–87.5)	
Within nERS	15 (21.43)	35 (36.84)		81 (77–85)	
By ERS			< 0.001#		0.225
Cleft 0	3 (5.45)	1 (1.67)		78.5 (76.75–81)	
Cleft 1–2	15 (27.27)	5 (8.33)		83.5 (78.75–86)	
Cleft 3	9 (16.36)	5 (8.33)		80 (69–83.75)	
Cleft 4	2 (3.64)	0 (0.00)		85 (84.5–85.5)	
Cleft 5	2 (3.64)	2 (3.33)		82.5 (81.75–85)	
Cleft 6	0 (0.00)	0 (0.00)		—	
Cleft 7	4 (7.27)	4 (6.67)		76.5 (70.75–86.5)	
Cleft 8	4 (7.27)	6 (10.00)		87 (80–92.25)	
Cleft 9	8 (14.55)	4 (6.67)		86.5 (83.25–91)	
Cleft 10	3 (5.45)	6 (10.00)		79 (74–89)	
Cleft 11	1 (1.82)	1 (1.67)		83 (81.5–84.5)	
Cleft 12	0 (0.00)	0 (0.00)		—	
Cleft 13	2 (3.64)	3 (5.00)		83 (79–91)	
Cleft 14	0 (0.00)	0 (0.00)		—	
Cleft 30	0 (0.00)	2 (3.33)		76.5 (75.75–77.25)	
Anterior neck midline (A.N.M.)	0 (0.00)	0 (0.00)		—	
Laterocervical line (L.L.)	1 (1.82)	4 (6.67)		71 (71–78)	
HM-FP	1 (1.82)	2 (3.33)		78 (78–79)	
FEFH-FP	0 (0.00)	15 (25.00)		83 (75.5–87)	
By nERS			0.003*		0.518
Forehead	1 (6.67)	3 (8.57)		82.5 (80–86.25)	
Cheek	10 (66.67)	10 (28.57)		81 (77.5–84)	
Chin	0 (0.00)	1 (2.86)		68 (68–68)	
Upper lip	0 (0.00)	0 (0.00)		—	
Lower lip	3 (20.00)	4 (11.43)		83 (78–87)	
Neck	0 (0.00)	1 (2.86)		77 (77–77)	
Eyelid	0 (0.00)	0 (0.00)		—	
Nose	1 (6.67)	0 (0.00)		73 (73–73)	
Ear	0 (0.00)	16 (45.71)		81.5 (77–86)	

* $P < 0.05$; # $P < 0.001$. Gender analyses: Women, count (%) of women with SCC in a specific site; men, count (%) of men with SCC in a specific site. Age analyses: site, median (25th–75th percentiles) of age distribution in specific sites. FEFH-FP, free ear fold-hyoid fusion plane; HM-FP, hyoid-mandibular fusion plane.

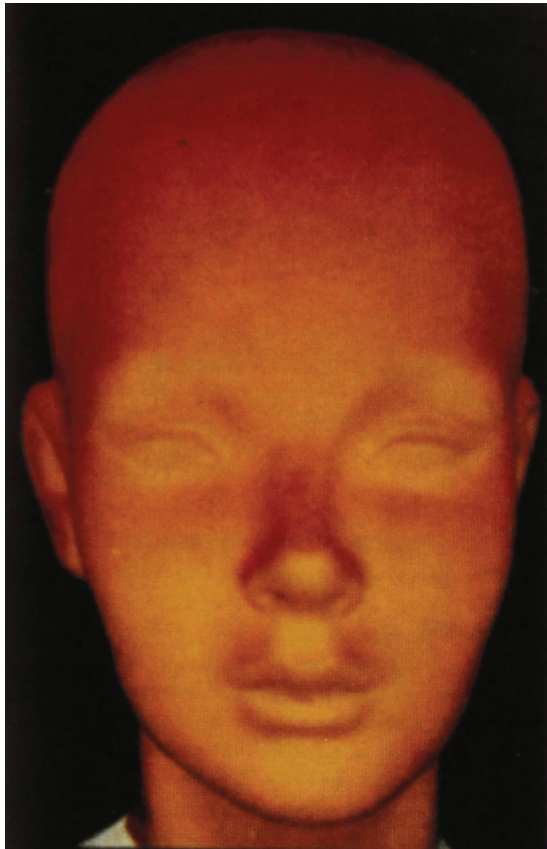


Fig. 7. Distribution of UV exposure on a coated manikin with a chemical ultraviolet dosimeter. Lighter-colored areas indicate less sun exposure. Reprinted with permission from Elsevier from: Urbach F. Geographic pathology of skin cancer. In: *Biologic effects of ultraviolet radiation (with emphasis on skin)*. Oxford Pergamon Press ©1969: 643.

where a process yielding to the development of an NMSC might take place. The chance of a BCC to develop within an ERS is 5-fold higher than an SCC. The environmental UV exposure plays a relatively main role versus dysontogenetic factors in the pathogenesis of SCC.

Giovanni Nicoletti, MD, FEBOPRAS

Plastic and Reconstructive Surgery

Department of Clinical Surgical Diagnostic and Pediatric Sciences

University of Pavia

Viale Brambilla, 74

27100 Pavia, Italy

Phone: +39 0382 984184

Fax: +39 0382 984055

E-mail: giovanni.nicoletti@unipv.it

REFERENCES

1. Mancebo SE, Wang SQ. Skin cancer: role of ultraviolet radiation in carcinogenesis. *Rev Environ Health*. 2014;29:265–273.
2. DIX CR. Occupational trauma and skin cancer. *Plast Reconstr Surg Transplant Bull*. 1960;26:546–554.
3. Sinha S, Su S, Workentine M, et al. Transcriptional analysis reveals evidence of chronically impeded ECM turnover and

epithelium-to-mesenchyme transition in scar tissue giving rise to Marjolin's ulcer. *J Burn Care Res*. 2017;38:e14–e22.

4. Poccia I, Persichetti P, Marangi GF, et al. Basal cell carcinoma arising in a chronic venous ulcer: two cases and a review of the literature. *Wounds*. 2014;26:30–35.
5. Azizova TV, Bannikova MV, Grigoryeva ES, et al. Risk of malignant skin neoplasms in a cohort of workers occupationally exposed to ionizing radiation at low dose rates. *PLoS One*. 2018;13:e0205060.
6. Lee CH, Liao WT, Yu HS. Aberrant immune responses in arsenical skin cancers. *Kaohsiung J Med Sci*. 2011;27:396–401.
7. Sanches MM, Travassos AR, Soares-de-Almeida L. [The relationship between immunodepression and the development of skin cancer]. *Acta Med Port*. 2017;30:69–72.
8. Nicoletti G, Brenta F, Malovini A, et al. Sites of basal cell carcinomas and head and neck congenital clefts: topographic correlation. *Plast Reconstr Surg Glob Open*. 2014;2:e164.
9. Nicoletti G, Tresoldi MM, Malovini A, et al. Correlation between the sites of onset of basal cell carcinoma and the embryonic fusion planes in the auricle. *Clin Med Insights Oncol*. 2018;12:1179554918817328.
10. Tessier P. Anatomical classification facial, cranio-facial and latero-facial clefts. *J Maxillofac Surg*. 1976;4:69–92.
11. Moore MH, David DJ, Cooter RD. Hairline indicators of cranio-facial clefts. *Plast Reconstr Surg*. 1988;82:589–593.
12. Jellouli Elloumi A, Souissi R, Trabelsi A, et al. [Congenital cysts and fistulas of the face and neck: often unrecognized dysembryoplasias]. *Tunis Med*. 1999;77:117–126.
13. Stricker M, Flot F, Malka G, et al. [Cysts and fistulas of embryonal origin of the face]. *Rev Stomatol Chir Maxillofac*. 1976;77:109–112.
14. Beauvillain de Montreuil C, Hamon S, Litoux P. Congenital cysts and fistulae of the face and the neck. *Ann Dermatol Venerol*. 1988;115:855–858.
15. Lachard J, Gola R. [Congenital cysts and fistulas of the neck]. *Rev Prat*. 1983;33:1557–1563.
16. González-Ulloa M. Regional aesthetic units of the face. *Plast Reconstr Surg*. 1987;79:489–490.
17. Fattahi TT. An overview of facial aesthetic units. *J Oral Maxillofac Surg*. 2003;61:1207–1211.
18. Urbach F. The historical aspects of photocarcinogenesis. *Front Biosci*. 2002;7:e85–e90.
19. Blaschko A. Die Nervenverteilung in der Haut in ihrer Beziehung zu den Erkrankungen der Haut. In: *Beilage Zu Den Verhandlungen Der Deutschen Dermatologischen Gesellschaft. VII Congress zu Breslau*. Mai. Wien, Leipzig: Braumüller; 1901.
20. Jackson R. The lines of Blaschko: a review and reconsideration: observations of the cause of certain unusual linear conditions of the skin. *Br J Dermatol*. 1976;95:349–360.
21. Newman JC, Leffell DJ. Correlation of embryonic fusion planes with the anatomical distribution of basal cell carcinoma. *Dermatol Surg*. 2007;33:957–64; discussion 965.
22. Lever WF. Pathogenesis of benign tumors of cutaneous appendages and of basal cell epithelioma. *Arch Derm Syphilol*. 1948;57:679–724.
23. Mehregan AH, pinkus H. Life history of organoid nevi. Special reference to nevus sebaceus of Jadassohn. *Arch Dermatol*. 1965;91:574–588.
24. Mason JK, Helwig EB, Graham JH. Pathology of the nevoid basal cell carcinoma syndrome. *Arch Pathol*. 1965;79:401–408.
25. Pinkus H. Adnexal tumors, benign, not-so-benign and malignant. *Adv Biol Skin*. 1966;7:255–276.
26. Nüsslein-Volhard C, Wieschaus E. Mutations affecting segment number and polarity in drosophila. *Nature*. 1980;287:795–801.
27. Wu F, Zhang Y, Sun B, et al. Hedgehog signaling: from basic biology to cancer therapy. *Cell Chem Biol*. 2017;24:252–280.

28. Caro I, Low JA. The role of the hedgehog signaling pathway in the development of basal cell carcinoma and opportunities for treatment. *Clin Cancer Res*. 2010;16:3335–3339.
29. Sandhiya S, Melvin G, Kumar SS, et al. The dawn of hedgehog inhibitors: vismodegib. *J Pharmacol Pharmacother*. 2013;4:4–7.
30. Metzis V, Courtney AD, Kerr MC, et al. Patched1 is required in neural crest cells for the prevention of orofacial clefts. *Hum Mol Genet*. 2013;22:5026–5035.
31. Abramyan J. Hedgehog signaling and embryonic craniofacial disorders. *J Dev Biol*. 2019;7:E9.
32. Pellegrini C, Maturo MG, Di Nardo L, et al. Understanding the molecular genetics of basal cell carcinoma. *Int J Mol Sci*. 2017;18:E2485.
33. Jackson R. Geographic pathology of skin cancer. *J Cutan Med Surg*. 1999;3:120–122.
34. Urbach F. Geographic pathology of skin cancer. In: Urbach F, ed. *Biological Effects of Ultraviolet Radiation (With Emphasis on Skin)*. Oxford Pergamon Press; 1969:635–653.
35. Frampton JE, Basset-Séguin N. Vismodegib: a review in advanced basal cell carcinoma. *Drugs*. 2018;78:1145–1156.